

Hierarchical Probabilistic Forecasting of Electricity Demand with Smart Meter Data

Souhaib Ben Taieb

Department of Computer Science, University of Mons *

James W. Taylor

Saïd Business School, University of Oxford

and

Rob J. Hyndman

Department of Econometrics and Business Statistics, Monash University

February 21, 2020

Abstract

Decisions regarding the supply of electricity across a power grid must take into consideration the inherent uncertainty in demand. Optimal decision-making requires probabilistic forecasts for demand in a hierarchy with various levels of aggregation, such as substations, cities and regions. The forecasts should be coherent in the sense that the forecast of the aggregated series should equal the sum of the forecasts of the corresponding disaggregated series. Coherency is essential, since the allocation of electricity at one level of the hierarchy relies on the appropriate amount being provided from the previous level. We introduce a new probabilistic forecasting method for a large hierarchy based on UK residential smart meter data. We find our method provides coherent and accurate probabilistic forecasts, as a result of an effective forecast combination. Furthermore, by avoiding distributional assumptions, we find that our method captures the variety of distributions in the smart meter hierarchy. Finally, the results confirm that, to ensure coherency in our large-scale hierarchy, it is sufficient to model a set of lower-dimension dependencies, rather than modeling the entire joint distribution of all series in the hierarchy. In achieving coherent and accurate hierarchical probabilistic forecasts, this work contributes to improved decision-making for smart grids.

Keywords: Aggregates of time series; Empirical copulas; Forecast combinations; Predictive distributions; Smart meters

*Souhaib is an Adjunct Senior Research Fellow in the Department of Econometrics and Business Statistics, Monash University.

1 Introduction

Forecasts of electricity demand are needed for the efficient and secure management of power grids. Traditionally, the focus has been on forecasting the demand for the whole system. However, this is changing due to the increasing adoption of smart meters, which provide an accurate record of electricity consumption within intraday periods at the level of individual commercial and residential properties (Borenstein & Bushnell 2015). Along with detailed data regarding power generation, smart meters provide the basis of smart grids, which enable electricity consumption to be managed in a dynamic, efficient, reliable and sustainable way (Ramchurn et al. 2012, Mirowski et al. 2014). Demand forecasts are important for various levels of aggregation of the individual consumers. For example, grid management can benefit from the availability of predictions at the level of individuals, transformers, feeders, substations, balancing areas, cities, regions, and countries (Smith et al. 2010, Cho et al. 2013, Haben et al. 2014, Sun et al. 2016, Cabrera & Schulz 2017). In this context, the forecasting problem involves a hierarchy of time series, with levels consisting of differing degrees of aggregation.

Forecasting a hierarchy of time series presents a number of challenges. First, the series at different levels of the hierarchy, corresponding to different degrees of aggregation, can exhibit notably different features. While smart meter data is characterized by intermittency, relatively high volatility, and skewness, aggregated series will naturally be more smoothly evolving, less skewed, and show clearer signs of seasonality and weather-dependency. These differences have implications for the choice of forecasting method to use at different levels of the hierarchy. Forecasts for the aggregates could be produced by simply summing forecasts of the corresponding series at the lower levels. However, this bottom-up approach generally delivers poor results (Hyndman et al. 2011). This links to a second significant challenge, which is the requirement that the forecast of each aggregated series should equal the sum of the forecasts of the corresponding disaggregated series, in order to support coherent decision-making at different levels of the hierarchy. This aggregation constraint is unlikely to be satisfied if the forecasts for each series in the hierarchy are produced independently. Lastly, in many applications, such as the smart meter context, the hierarchy can consist of thousands, or even millions, of time series at the bottom level, which has implications for the choice of forecasting method in terms of computational load.

Generating forecasts to support decision-making in a hierarchical structure is important in many other applications, such as retail (Kremer et al. 2016) and tourism (Wickramasuriya et al. 2018). Recently proposed methods involve two stages, with forecasts first produced independently for each series in the hierarchy, and then combined to enable a synthesis of available information, and to ensure compliance with the aggregation constraint (see, for example, van Erven & Cugliari 2015). A notable feature of the hierarchical forecasting literature is the lack of probabilistic prediction. This is a significant limitation, because optimal decision making, in a variety of applications, requires an assessment of forecast uncertainty (see, for example, Berrocal et al. 2010, Jeon & Taylor 2012). In the electricity demand context, probabilistic predictions of the total system load are used for stochastic unit commitment models, power supply planning, setting operating reserve, price forecasting, and electricity market trading (Hong et al. 2016). With regard to disaggregated load, probabilistic forecasts are used to ensure a balance between generation and consumption at regional (Cabrera & Schulz 2017) and distributional levels (Sun et al. 2016). At the smart meter level, suppliers can use probabilistic forecasts to update pricing and incentive schemes for individual customers (Arora & Taylor 2016, Ben Taieb et al. 2016). An advantage of generating probabilistic forecasts for the entire hierarchy is that it allows the possibility of predictions for each series in the hierarchy to benefit from the information elsewhere in the hierarchy.

We introduce an approach for producing a probability density forecast for each series within a large-scale hierarchy. Our aim is probabilistic forecasts that are “aggregate coherent”; i.e., the forecast distribution of each aggregate series is equal to the convolution of the forecast distributions of the corresponding disaggregate series. Such forecasts naturally satisfy the aggregation constraints of the hierarchy. Our method allows different types of distributions, and accounts for dependencies to enable the computation of the predictive distribution of the aggregates. It proceeds by independently generating a density forecast for each series in the hierarchy. Then, a state-of-the-art hierarchical forecast combining method is applied to produce revised coherent mean forecasts. Samples are then taken from the densities. Drawing on the work of Arbenz et al. (2012), a set of permutations, derived from empirical copulas, are applied to the multivariate samples to restore dependencies before computing the sums corresponding to the aggregates in the hierarchy. The result is aggregate coherent density forecasts for the entire hierarchy.

Our approach has four advantages. First, for every series in the hierarchy, a density forecast

is produced, and these together satisfy the coherency constraints. Second, each estimated density and dependency structure is the result of a synthesis of information from different levels of the hierarchy. Third, distributional assumptions are not required. Fourth, the problem is decomposed into lower-dimension sub-problems, enabling the approach to be scalable to large hierarchies. We note that the paper by Borges et al. (2013) concerns the forecasting of a hierarchy with electricity load at the substation level. However, this paper differs from our focus because it does not deal with smart meter data, probabilistic forecasting or hierarchical coherency. Furthermore, the hierarchies considered are relatively small, consisting of just a top and bottom level.

Section 2 introduces the smart meter data that we analyze in this paper. Section 3 discusses hierarchical forecasting for the mean, while Section 4 presents our new approach to probabilistic hierarchical forecasting. For our smart meter data, Section 5 describes the forecasting methods that we implement for individual series in the hierarchy, and Section 6 presents forecasting results. Section 7 provides a simulation study, and Section 8 concludes the paper.

2 Smart Electricity Meter Data

Our empirical analysis involves time series of electricity consumption, recorded by smart meters at residential properties in Great Britain. The data was collected, along with geographic and demographic information, by four energy supply companies as part of a research project aimed at understanding domestic energy usage (AECOM Building Engineering 2014, AECOM 2011). Although more than 14000 series were available, for simplicity, we chose to avoid relatively short series with a lot of missing observations, and this led us to select data recorded at 1578 meters for the period of approximately 15 months from 20 April 2009 to 31 July 2010, inclusive. With the data recorded half-hourly, each series consisted of 22464 observations. In excluding short series with many missing observations, we were focusing on the sort of data that would be relevant to the existing hierarchical forecasting methods and our new proposals. For each series, we used the approximately 12 months up to 30 April 2010, for model estimation, and the final three calendar months for post-sample evaluation. Our interest is in predictions made each day from 23:30 for each half-hour of the next day, which implies 48 different lead times.

Using the geographical information, we constructed a hierarchy consisting of five levels. These

levels corresponded to the NUTS (Nomenclature of Territorial Units) statistical regions of the United Kingdom, with the top level being the East Midlands region of England, and the second level being the counties within that region. The five levels had the following numbers of series: 1578 (Level 5, the bottom level), 40 (Level 4), 11 (Level 3), 3 (Level 2), and 1 (Level 1, the top level). In total, therefore, the hierarchy consists of 1633 series, with 1578 in the bottom level and 55 aggregates in the other levels. The hierarchy's architecture is summarized in Figure 1, where each node corresponds to one of the aggregates in Levels 1 to 4, and its size is in proportion to the number of smart meters aggregated from the bottom level. To reflect reality, we have allowed quite large variation in the number of smart meters making up the different aggregates. In the following, we use the terms ‘node’ and ‘series’ interchangeably.

In Figure 2, we present a one-week period for a series taken from each level of the hierarchy. The values on the left hand side of the figure indicate the number of smart meter series that have been summed to give each aggregated series. The series from the higher levels show daily and weekly patterns, which become increasingly evident with greater aggregation. For example, the intraday patterns for Saturday and Sunday can be seen to be similar to each other, but different to the weekdays, for the top level series and the series formed from the aggregation of the 150 series. However, this is much less clear in the three other series in Figure 2. Indeed, daily and weekly patterns are not so apparent in the series from the bottom level, which exhibits relatively

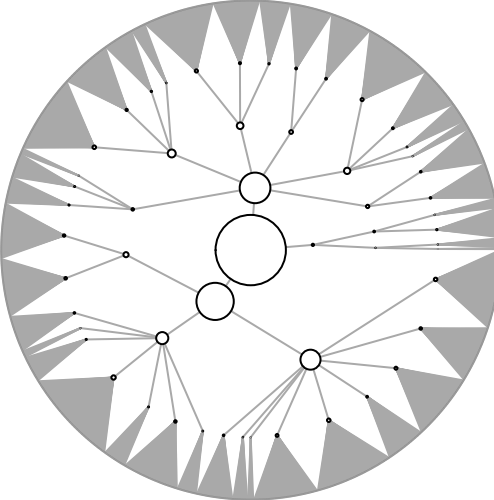


Figure 1: The hierarchical structure of the electricity network, where the size of each node is proportional to the number of aggregated meters.

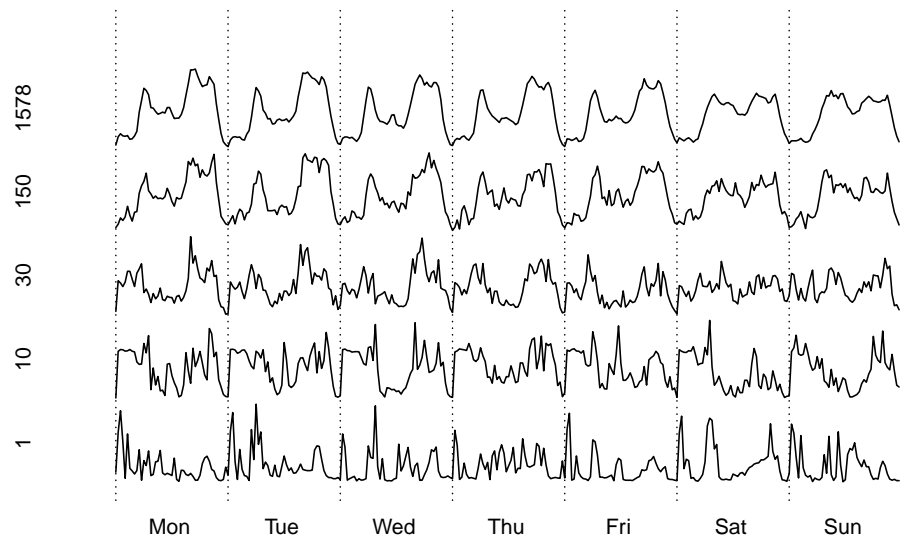


Figure 2: A one-week period of demand corresponding to different numbers of aggregated meters.

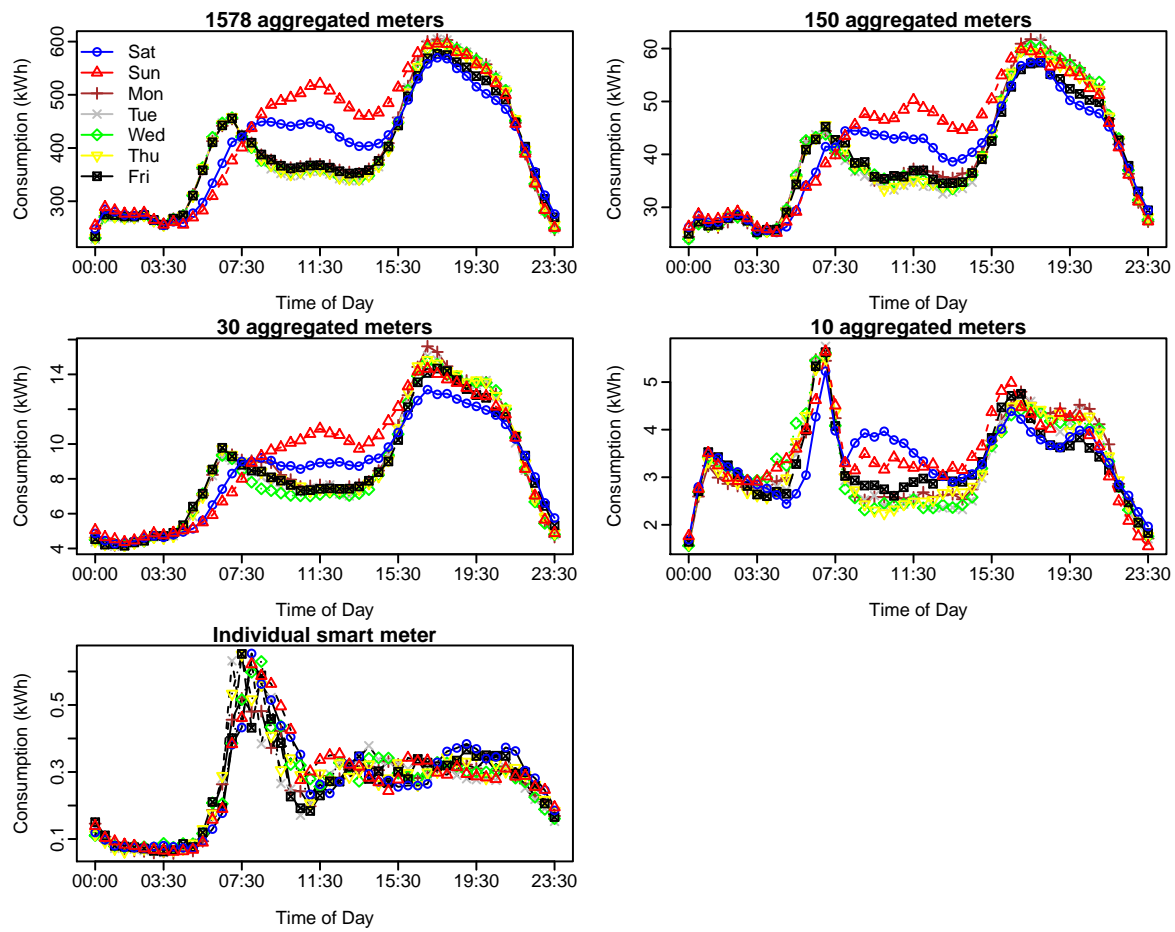


Figure 3: Intraday pattern for each day of the week and different numbers of aggregated meters.

volatile behavior, with occasional spikes, which suggests the distribution of consumption is positively skewed. For the same five series, Figure 3 shows the intraday pattern for each day of the week, averaged over the full series. It is interesting to see from Figure 3 the existence of cyclical patterns in the daily profiles for the individual smart meter series. For this particular household, the average daily pattern varies little across the seven days of the week.

3 Hierarchical Mean Electricity Demand Forecasting

In this section, we first introduce terminology and our notation relating to hierarchical forecasting. We then describe the method of Wickramasuriya et al. (2018), which has been introduced for mean hierarchical forecasting, but has the potential to be used for probabilistic hierarchical forecasting.

3.1 Hierarchical forecasting

Electricity consumption collected by smart meters, and the associated aggregated consumption form a multivariate time series with a hierarchical structure, also called a hierarchical time series. Building on the notation in Hyndman et al. (2016), we let \mathbf{b}_t be an m -vector with the observations at time t in the bottom level. Then, the r -vector with the observations at the different levels of aggregation is given by $\mathbf{a}_t = \mathbf{A}\mathbf{b}_t$ where the matrix $\mathbf{A} \in \{0, 1\}^{r \times m}$, and $t = 1, \dots, T$. An entry of \mathbf{A} is equal to 1 if the associated bottom-level observation is included in the aggregation. Finally, we let $\mathbf{y}_t = (\mathbf{a}_t \ \mathbf{b}_t)'$ be an n -vector containing observations both at the bottom and aggregate levels, given by $\mathbf{y}_t = \mathbf{S}\mathbf{b}_t$, where $\mathbf{S}' = [\mathbf{A}' \ \mathbf{I}_m] \in \{0, 1\}^{n \times m}$ and \mathbf{I}_m is an identity matrix of order m . To avoid pathological hierarchies, we will assume that $m > 0$, $r > 0$ and $\sum_{j=1}^r s_{ij} > 1$ where s_{ij} is the entry in the i th row and j th column of matrix \mathbf{S} . Figure 4 gives a small example with $m = 5$ bottom level series with $\mathbf{b}_t = (y_{aa,t}, y_{ab,t}, y_{ba,t}, y_{bb,t}, y_{bc,t})'$, and $r = 3$ aggregate series with $\mathbf{a}_t = (y_t, y_{a,t}, y_{b,t})'$.

Given historical observations $\mathbf{y}_1, \dots, \mathbf{y}_T$, forecasting the mean electricity consumption for each half-hour h of the next day reduces to estimating the h period-ahead conditional expectation:

$$\mathbb{E}[\mathbf{y}_{T+h} | \mathbf{y}_1, \dots, \mathbf{y}_T] = \mathbf{S} \mathbb{E}[\mathbf{b}_{T+h} | \mathbf{b}_1, \dots, \mathbf{b}_T], \quad (1)$$

where $h = 1, 2, \dots, 48$. Recall that our interest is in predictions made each day from 23:30 for each

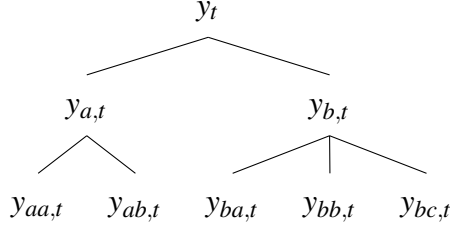


Figure 4: Example of a hierarchical time series.

half-hour of the next day, implying 48 lead times.

A natural plug-in estimator for expression (1), known as *bottom-up*, is given by

$$\hat{\mathbf{y}}_{T+h} = \mathbf{S}\hat{\mathbf{b}}_{T+h}, \quad (2)$$

where $\hat{\mathbf{b}}_{T+h} = (\hat{b}_{1,T+h}, \dots, \hat{b}_{m,T+h})'$, $\hat{b}_{j,T+h}$ is an estimate of $\mathbb{E}[b_{j,T+h} | b_{j,1}, \dots, b_{j,T}]$, and $b_{j,t}$ denotes the j th variable of the vector \mathbf{b}_t with $j = 1, \dots, m$. In other words, the mean forecasts for each aggregate node are computed by summing the mean forecasts of the associated bottom level series. This approach is computationally efficient since it only requires summing bottom level forecasts. However, the series at the most disaggregated level often have a low signal-to-noise ratio, which makes them hard to predict. Indeed, this is the case for our electricity consumption hierarchy. Therefore, summing bottom level forecasts is unlikely to provide good forecast accuracy at upper levels in the hierarchy (Hyndman et al. 2011).

Another approach, known as *base*, forecasts all nodes at all levels independently. More precisely, we compute

$$\hat{\mathbf{y}}_{T+h} = (\hat{y}_{1,T+h}, \dots, \hat{y}_{n,T+h})' = (\hat{\mathbf{a}}'_{T+h} \hat{\mathbf{b}}'_{T+h})' \quad (3)$$

where $\hat{y}_{i,T+h}$ is an estimate of $\mathbb{E}[y_{i,T+h} | y_{i,1}, \dots, y_{i,T}]$ and $y_{i,t}$ denotes the i th variable of the vector \mathbf{y}_t with $i = 1, \dots, n$. This approach provides flexibility since we can use different forecasting algorithms for each series and aggregation level. However, the base forecasts $\hat{\mathbf{y}}_{T+h}$ will generally not satisfy the aggregation constraints, i.e. $\hat{\mathbf{a}}_{T+h} = \mathbf{A}\hat{\mathbf{b}}_{T+h}$, with the constraint violations for each aggregate series at horizon h given by

$$\tilde{\mathbf{e}}_{T+h} = \hat{\mathbf{a}}_{T+h} - \mathbf{A}\hat{\mathbf{b}}_{T+h}. \quad (4)$$

The forecasts $\hat{\mathbf{y}}_{T+h}$ in expression (3) are *mean coherent* if $\tilde{\boldsymbol{\epsilon}}_{T+h} = \mathbf{0}$, and are incoherent otherwise.

Since the optimal mean forecasts in expression (1) are coherent by definition, it seems sensible to impose the aggregation constraints when generating hierarchical mean forecasts. Furthermore, coherent forecasts will allow coherent decisions over the entire hierarchy.

Starting from a set of (probably incoherent) base forecasts $\hat{\mathbf{y}}_{T+h}$, Hyndman et al. (2011) proposes the computation of revised coherent hierarchical forecasts of the following form:

$$\tilde{\mathbf{y}}_{T+h} = \mathbf{S}\tilde{\mathbf{b}}_{T+h} \text{ and } \tilde{\mathbf{b}}_{T+h} = \mathbf{P}_h\hat{\mathbf{y}}_{T+h}, \quad (5)$$

for some appropriately chosen matrix $\mathbf{P}_h \in \mathbb{R}^{m \times n}$. In other words, forecasts are obtained by summing bottom level revised forecasts $\tilde{\mathbf{b}}_{T+h}$, which have been computed by combining forecasts from all levels $\hat{\mathbf{y}}_{T+h}$. An advantage of the forecast in expression (5) is that it involves the combination of the forecasts from all levels of the hierarchy, applied through the weight matrix \mathbf{P}_h . Furthermore, many hierarchical forecasting methods are represented as particular cases, including the bottom-up forecasts, for which $\mathbf{P}_h = [\mathbf{0}_{m \times r} \mid \mathbf{I}_{m \times m}]$. Finally, the forecasts are coherent by construction.

3.2 The MinT approach to hierarchical forecasting

Instead of using an arbitrary weight matrix \mathbf{P}_h , Wickramasuriya et al. (2018) propose the minimization of the sum of the error variances, and derive a closed-form expression, as in the following:

Theorem 1. (Adapted from Wickramasuriya et al. 2018) Let $\hat{\mathbf{e}}_{t+h} = \mathbf{y}_{t+h} - \hat{\mathbf{y}}_{t+h}$ be the h period-ahead base forecast errors for $t = 1, \dots, T$, and $\mathbf{W}_h = \mathbb{E}[\hat{\mathbf{e}}_{t+h}\hat{\mathbf{e}}_{t+h}']$, the corresponding positive definite covariance matrix. Then, assuming unbiased base forecasts,

1. the covariance matrix of the h period-ahead revised forecast errors is given by

$$\tilde{\mathbf{V}}_h = \mathbb{V}[\mathbf{y}_{t+h} - \tilde{\mathbf{y}}_{t+h}] = \mathbf{S}\mathbf{P}_h\mathbf{W}_h\mathbf{P}_h'\mathbf{S}', \quad (6)$$

2. the weight matrix \mathbf{P}_h of the unbiased revised forecasts, which minimizes the trace of $\tilde{\mathbf{V}}_h$, is

$$\mathbf{P}_h^* = (\mathbf{S}'\mathbf{W}_h^{-1}\mathbf{S})^{-1}\mathbf{S}'\mathbf{W}_h^{-1}, \quad (7)$$

3. the revised forecasts of the mean are given by

$$\tilde{\mathbf{y}}_{T+h} = \mathbf{S}\mathbf{P}_h^*\hat{\mathbf{y}}_{T+h}. \quad (8)$$

We refer to this method as *MinT*, as it involves the minimization of the trace. Computing the matrix \mathbf{P}_h^* in expression (7) requires the estimation of the possibly high-dimensional covariance matrix \mathbf{W}_h or its inverse. However, \mathbf{W}_h is typically hard to estimate for $h > 1$. For example, an empirical approach has the problem that successive multi-step-ahead errors will not be independent for $h > 1$. We will assume $\mathbf{W}_h \propto \mathbf{W}_1$ (as in Wickramasuriya et al. 2018). For $h = 1$, the sample covariance matrix is given by

$$\hat{\mathbf{W}}_1 = \frac{1}{T} \sum_{t=1}^T \hat{\mathbf{e}}_t \hat{\mathbf{e}}_t',$$

where $\hat{\mathbf{e}}_t$ are the residuals (the in-sample one-step forecast errors) from the base models applied to each node in the hierarchy. However, since electricity demand volatility varies with the time of day, we will allow \mathbf{W}_1 to change for each half-hour s , $s = 1, \dots, 48$; i.e. we compute

$$\hat{\mathbf{W}}_{1,s} = \frac{\sum_t \mathbb{1}\{\lfloor t/48 \rfloor = s\} \hat{\mathbf{e}}_t \hat{\mathbf{e}}_t'}{\mathbb{1}\{\lfloor t/48 \rfloor = s\}}$$

where $\mathbb{1}\{\cdot\}$ is the indicator function, and $\lfloor \cdot \rfloor$ denotes the floor operator.

When $T = \mathcal{O}(n)$, the sample covariance matrix is singular, and hence not invertible. Consequently, Wickramasuriya et al. (2018) proposed using either a diagonal estimate, which ignores all covariances, or the regularized estimate of Schäfer & Strimmer (2005), which involves shrinking the off-diagonal terms of the sample covariance estimate towards zero. We call these *MinTDiag* and *MinTShrink*, respectively.

4 Hierarchical Probabilistic Electricity Demand Forecasting

In this section, we first introduce our definition for probabilistically coherent hierarchical forecasts. We then discuss how copulas provide a convenient framework to compute the distribution of the sum of random variables. Following that, we present a copula-based hierarchical probabilistic forecasting approach, and then describe how we implement an empirical copula through a set of

permutations. Finally, we present our new hierarchical probabilistic forecasting algorithm.

4.1 Probabilistically coherent hierarchical forecasts

Let $y_{i,t}$ denote the i th variable of the vector \mathbf{y}_t with $i = 1, \dots, n$. Recall that n is the number of nodes in the hierarchy, and is, therefore, the number of time series that need predicting. Instead of estimating the conditional mean given in expression (1), we want to estimate, for each node in the hierarchy, the h period-ahead conditional cumulative distribution function: $F_{i,T+h}(y | \mathbf{y}_1, \dots, \mathbf{y}_T) = \mathbb{P}(y_{i,T+h} \leq y | \mathbf{b}_1, \dots, \mathbf{b}_T)$ for each half-hour $h = 1, \dots, 48$.

Let $\hat{F}_{\mathbf{b},T+h}$ be the joint predictive distribution for \mathbf{b}_{T+h} ; $\hat{F}_{a_j,T+h}$ the predictive distribution for $a_{j,T+h}$; \mathbf{s}_j the j th row vector of matrix \mathbf{S} , for $j = 1, \dots, r$; and let $\stackrel{d}{=}$ denote equality in distribution. When $a_{j,T+h} \stackrel{d}{=} \mathbf{s}_j \mathbf{b}_{T+h}$, we describe the forecasts as *probabilistically coherent*. Note that if the forecasts are probabilistically coherent, they are also mean coherent.

It is possible to compute independently probabilistic base forecasts for each series: $F_{i,T+h}(y | y_{i,1}, \dots, y_{i,T}) = \mathbb{P}(y_{i,T+h} \leq y | y_{i,1}, \dots, y_{i,T})$. However, producing a forecast for each node, using only historical observations for that node, does not exploit the possible dependencies between the time series for different nodes. Furthermore, the probabilistic forecasts will not necessarily be probabilistically coherent due to estimation errors and possible model differences.

The MinT method of Theorem 1 allows for both coherent mean forecasts $\tilde{\mathbf{y}}_{T+h}$ given in expression (8), and the calculation of the associated forecast variances $\tilde{\mathbf{V}}_h$ given in expression (6). Therefore, for the situation where the distribution is completely specified by its first two moments, it is possible to produce coherent probabilistic forecasts. In the case of electricity demand, forecast distributions tend to be highly skewed, and so one option is to assume a log-normal distribution, as this is completely specified by its first two moments. In this paper, we avoid distributional assumptions, as we do not want to restrict the choice of forecasting method used for any individual series. Our proposal uses a bottom-up approach based on Monte Carlo sampling of the bottom level predictive distributions. We use the MinT approach to adjust the mean of each of the bottom level distributions, and then account for dependencies using empirical copulas (Rüschendorf 2009).

4.2 Copula-based distribution of sums of random variables

Since each aggregate node is the sum of a subset of bottom level nodes, computing bottom-up predictive distributions reduces to computing the distribution of sums of random variables. Let us first focus on a simple hierarchy with d bottom level nodes and one aggregate node, and only consider unconditional distributions. Let $\mathbf{X} = (X_1, \dots, X_d)$ be a random vector with continuous marginals F_i , and joint distribution F . The distribution of $Z = \sum_{i=1}^d X_i$ at value z is given by

$$F_Z(z) = \int_{\mathbb{R}^d} \mathbb{1}\{x_1 + \dots + x_d \leq z\} dF(x_1, \dots, x_d), \quad (9)$$

where $(x_1, \dots, x_d) \in \mathbb{R}^d$. Clearly, computing the distribution of the sum requires the joint distribution. In our application, the bottom level marginal predictive distributions \hat{F}_i are available. To take advantage of this, instead of directly estimating the joint distribution F , it seems appealing to employ a forecasting algorithm that uses the predictive marginals \hat{F}_i to estimate the joint distribution F . A natural and convenient framework to enable this is provided by copulas (Nelsen 2007).

Copulas originate from Sklar's theorem (Sklar 1959), which states that for any continuous distribution function F with marginals F_1, \dots, F_d , there exists a unique “copula” function $\mathbf{C} : [0, 1]^d \rightarrow [0, 1]$ such that F can be written as $F(x_1, \dots, x_d) = C(F_1(x_1), \dots, F_d(x_d))$. This allows us to decouple the computation of the marginal predictive distributions from the computation of the dependence structure. Since we are interested in multivariate forecasting, we will need a version of Sklar's theorem for conditional distributions proposed by Patton (2006). Given some information set \mathcal{F}_{t-1} , if $\mathbf{y}_t | \mathcal{F}_{t-1} \sim F(\cdot | \mathcal{F}_{t-1})$ with $y_{i,t} | \mathcal{F}_{t-1} \sim F_i(\cdot | \mathcal{F}_{t-1})$, $i = 1, \dots, d$, then

$$F(\mathbf{y} | \mathcal{F}_{t-1}) = C(F_1(y_1 | \mathcal{F}_{t-1}), \dots, F_d(y_d | \mathcal{F}_{t-1}) | \mathcal{F}_{t-1}). \quad (10)$$

In the following, we will omit the conditioning variables in order to simplify the notations,

4.3 A copula-based bottom-up procedure

Consider the hierarchy of Figure 4. If we compute the marginals for all bottom level nodes, i.e. $\hat{F}_{aa,t}, \hat{F}_{ab,t}, \hat{F}_{ba,t}, \hat{F}_{bb,t}, \hat{F}_{bc,t}$ and the associated five-dimensional copula \hat{C} , then the joint distribution \hat{F} can be computed using expression (10).

Although it is convenient to decouple the computation of the marginals from the computation of the dependence function, it is still challenging to specify a d -dimensional copula when d is large, which is indeed the case in our application where d is the number of households. Furthermore, with highly disaggregated time series data, the bottom level series often have a small signal-to-noise ratio making it difficult to estimate the dependence structure between the series.

However, since we are only interested in specific aggregations, we can avoid explicitly modeling the (often) high-dimensional copula that describes the dependence between all bottom level nodes. Similar to Arbenz et al. (2012), we decompose the problem into the estimation of multiple lower-dimensional copulas for all child nodes of each aggregate node (i.e. the nodes directly connected to the aggregate node), and compute the sum distribution in a hierarchical manner.

For the example in Figure 4, the following procedure allows us to compute the distributions of all aggregates in a hierarchical manner:

1. Compute $\hat{F}_{a,t}(\cdot)$ using $\hat{C}_1(\hat{F}_{aa,t}(\cdot), \hat{F}_{ab,t}(\cdot))$.
2. Compute $\hat{F}_{b,t}(\cdot)$ using $\hat{C}_2(\hat{F}_{ba,t}(\cdot), \hat{F}_{bb,t}(\cdot), \hat{F}_{bc,t}(\cdot))$.
3. Compute $\hat{F}_t(\cdot)$ using $\hat{C}_3(\hat{F}_{a,t}(\cdot), \hat{F}_{b,t}(\cdot))$.

Instead of computing a five-dimensional copula \hat{C} for all bottom level nodes in Figure 4, the hierarchical procedure uses three lower-dimensional copulas \hat{C}_1 , \hat{C}_2 and \hat{C}_3 for $(y_{aa,t}, y_{ab,t})$, $(y_{ba,t}, y_{bb,t}, y_{bc,t})$ and $(y_{a,t}, y_{b,t})$, respectively. Furthermore, by contrast with a simple bottom-up procedure, which uses information from only the bottom level, our approach conditions on information at multiple levels, which can be beneficial, as the series at the higher levels are smoother, and easier to model.

4.4 Empirical copulas and permutations

With the exception of some special cases where the distribution of the sum in expression (9) can be computed analytically, we would typically resort to Monte Carlo simulation (Gijbels & Herrmann 2014). Suppose we have samples $x_k^i \sim F_i$, and $\mathbf{u}_k = (u_k^1, \dots, u_k^d) \sim C$ with $i = 1, \dots, d$ and $k = 1, \dots, K$, then we can compute the empirical marginals

$$\hat{F}_i(x) = \frac{1}{K} \sum_{k=1}^K \mathbb{1}\{x_k^i \leq x\},$$

and the empirical copula

$$\hat{C}(\mathbf{u}) = \frac{1}{K} \sum_{k=1}^K \mathbb{1} \left\{ \frac{\text{rk}(u_k^1)}{K} \leq u_1, \dots, \frac{\text{rk}(u_k^d)}{K} \leq u_d \right\}, \quad (11)$$

for $\mathbf{u} = (u_1, \dots, u_d) \in [0, 1]^d$, where $\text{rk}(u_k^i)$ is the rank of u_k^i within the set $\{u_1^i, \dots, u_K^i\}$. Then, by Sklar's theorem, the joint distribution can be computed using expression (10).

The procedure of applying empirical copulas to empirical marginals is convenient since it can be efficiently represented in terms of sample reordering. Indeed, this can be seen by rewriting expression (10) using expression (11), and by exploiting the fact that $\hat{F}_i^{-1}(k/K) = x_{(k)}^i$ where $x_{(k)}^i$ denotes the order statistics of $\{x_1^i, \dots, x_K^i\}$. In other words, the order statistics $u_{(1)}^i, \dots, u_{(K)}^i$ of the samples u_1^i, \dots, u_K^i induce a permutation p_i of the integers $\{1, 2, \dots, K\}$, defined by $p_i(k) = \text{rk}(u_k^i)$ for $k = 1, \dots, K$, where a permutation denotes a bijective mapping from $\{1, 2, \dots, K\}$ to $\{1, 2, \dots, K\}$. If we apply the permutations to each independent marginal sample $\{x_1^i, \dots, x_K^i\}$, the reordered samples inherit the multivariate rank dependence structure from the copula \hat{C} .

Introducing a dependence structure into originally independent marginal samples goes back to Iman & Conover (1982) who considered the special case of normal copulas. Under appropriate regularity conditions, Mainik (2015) showed that the estimate of the distribution of the sum, computed using the reordering procedure, is strongly uniformly consistent with convergence rate $\mathcal{O}_p(T^{-1/2})$ where T is the sample size. The use of a sample reordering procedure to specify multivariate dependence structure has been considered in Arbenz et al. (2012) for high-dimensional risk aggregation, and by Schefzik et al. (2013) with applications to weather forecasting.

4.5 An algorithm for hierarchical probabilistic forecasting

In this section, we present the different steps of our algorithm, which produces probabilistic forecasts for a hierarchy with n series for lead times from one to H steps ahead.

Our algorithm generates random samples for all nodes in the hierarchy by applying a hierarchical reordering procedure on independent samples from all bottom-level nodes as explained in Section 4.3 and 4.4. Finally, a mean forecast combination is applied using the MinT method described in Section 3.2. The different steps of our algorithm are given below.

1. For each series $i = 1, \dots, n$, fit the base model and compute the in-sample base predictive distribution $\hat{F}_{i,t}$ for $t = 1, \dots, T$. Then, compute $u_{i,t} = \hat{F}_{i,t}(y_{i,t})$ and define the permutations $p_i(t) = \text{rk}(u_{i,t})$ as explained in Section 4.4, where $\text{rk}(u_{i,t})$ is the rank of $u_{i,t}$ within the set $\{u_{i,1}, \dots, u_{i,T}\}$. Note that it is possible to allow the copula (and the associated permutations) to vary for each half-hour. However, we did not find this beneficial, and this can be explained by the fact that we are already conditioning by half-hour for the marginals.
2. Let $\hat{\mathbf{y}}_t = (\hat{y}_{1,t}, \dots, \hat{y}_{n,t})'$, where $\hat{y}_{i,t}$ is the mean of the in-sample base predictive distribution $\hat{F}_{i,t}$. Compute the covariance matrix $\hat{\mathbf{W}}_1$ of the base forecast errors $\hat{\mathbf{e}}_t = \mathbf{y}_t - \hat{\mathbf{y}}_t$ as explained in Section 3.2, and compute the MinT combination weight matrix $\hat{\mathbf{P}}_h$ given by expression (7).
3. For each series $i = 1, \dots, n$ and each horizon $h = 1, \dots, H$, compute an h period-ahead post-sample base predictive distribution $\hat{F}_{i,T+h}$. Compute the revised mean forecasts $\tilde{\mathbf{y}}_{T+h} = \hat{\mathbf{S}}\hat{\mathbf{P}}_h\hat{\mathbf{y}}_{T+h}$, where $\hat{\mathbf{P}}_h$ has been previously computed using the MinT approach in step 2 and $\hat{\mathbf{y}}_{T+h} = (\hat{y}_{1,T+h}, \dots, \hat{y}_{n,T+h})'$, where $\hat{y}_{i,T+h}$ is the post-sample base predictive mean of $y_{i,T+h}$.
4. For each bottom level node $i = r+1, \dots, n$, produce a sample of size K , x_1^i, \dots, x_K^i , with

$$x_k^i = \tilde{F}_{i,T+h}^{-1}(\tau_k), \quad (12)$$

where

$$\tilde{F}_{i,T+h}^{-1}(\tau_k) = \hat{F}_{i,T+h}^{-1}(\tau_k) - \hat{y}_{i,T+h} + \tilde{y}_{i,T+h}, \quad (13)$$

$\tau_k \sim U(0, 1)$ and $k = 1, \dots, K$. In other words, x_1^i, \dots, x_K^i is a sample from the base predictive distribution $\hat{F}_{i,T+h}$ with revised predictive mean $\tilde{y}_{i,T+h}$.

5. For each aggregate node $i = 1, \dots, r$, produce a sample of size K , x_1^i, \dots, x_K^i , by recursively computing

$$x_k^i = x_{(p_{c(i,1)}(k))}^{c(i,1)} + \dots + x_{(p_{c(i,n_i)}(k))}^{c(i,n_i)}, \quad (14)$$

where $c(i, j)$ is the j th child node of the aggregate node i , where $j = 1, \dots, n_i$, and $x_{(k)}^i$ denotes the k th order statistic of $\{x_1^i, \dots, x_K^i\}$, i.e. $x_{(1)}^i \leq \dots \leq x_{(K)}^i$. In other words, in expression (14), for each aggregate node, we first apply the permutations computed in step 1 to the

independent samples of the child nodes generated using expression (12). A sample for the aggregate node is then obtained by summing the permuted samples.

Note that we have used the T historical observations to compute the permutations in step 1. When $K \neq T$, in order to apply the permutations to the independent sample of size K , we can generate a bootstrap sample from the T permutations. If a parametric copula is fitted, we can generate a sample of size K from the estimated copula.

Compared to a simple bottom-up approach, which uses information from only the bottom level, our algorithm synthesizes information from multiple levels. In particular, we apply the MinT approach to revise the mean forecasts, which allows us to take advantage of more accurate forecasts of the mean at higher levels. Furthermore, we estimate the permutations at different aggregate levels, which allows us to benefit from better estimation since the series are smoother, and hence easier to model. Finally, compared to MinT, our approach does not require distributional assumptions.

5 Forecasting Individual Electricity Demand Series

The first step of our proposed hierarchical probabilistic forecasting algorithm involves independently generating density forecasts for each series in the hierarchy. In this section, we present the density forecasting methods that we applied to each individual series. In the hierarchical forecasting context, these are termed the *base* forecasting methods. In choosing methods to use for the base forecasts, we draw on the literature on forecasting electricity consumption. We do not develop new methods for base forecasting, because our contribution in this paper relates to the different problem of converting any set of base forecasts into a hierarchy of potentially more accurate forecasts that are probabilistically coherent.

Hong et al. (2016) describe how there are many different approaches available for probabilistic forecasting of the total electricity demand on a transmission system. For day-ahead prediction, a weather-based model is typically used (see, for example, Cottet & Smith 2003, Smith et al. 2010, Cho et al. 2013). For shorter lead times, univariate time series models have been proposed (see, for example, De Livera et al. 2011), and from these, density forecasting is straightforward. This contrasts with weather-based models, for which the generation of probabilistic demand forecasts

requires density forecasts for the weather variables (Taylor & Buizza 2002). As our focus is on large-scale hierarchical forecasting, rather than the modeling of individual time series, for simplicity, we use univariate methods. Because the series in the bottom level of the hierarchy exhibit different features to the aggregate series, we use different forecasting methods for each.

5.1 Forecasting bottom level series

For our smart meter series, the non-Gaussian behavior and lack of clear autoregressive structure (see, for example, Figure 2) motivates a nonparametric approach to density forecasting. This is supported by the results of Arora & Taylor (2016), who found that, for residential smart meter series, several kernel density estimation (KDE) approaches outperformed exponential smoothing. We implemented the best performing of those KDE approaches (see Section 3.7 of Arora & Taylor 2016) for our smart meter series, which constitute the bottom level of our hierarchy.

This KDE approach has the appeal of simplicity, which is important because, in a smart meter application, it would typically need to be applied within an automated procedure. The approach treats the five weekdays as identical, and applies KDE separately to the 48 half-hours of the day. It treats Saturday and Sunday as different, and again performs KDE separately for each period of the day. The days of the week are, therefore, categorized into three different day types. Using historical observations y_1, \dots, y_T , the predictive density at value y for period $T + h$ is expressed as:

$$\hat{f}_{T+h}(y) = \frac{\sum_{t \in S_{T+h}} \lambda^{\lfloor (T-t)/336 \rfloor} K_b(y_t - y)}{\sum_{t \in S_{T+h}} \lambda^{\lfloor (T-t)/336 \rfloor}},$$

where $K_b(\cdot) = K(\cdot/b)/b$ denotes a kernel function with bandwidth b ; S_{T+h} is the set of past periods that fall on the same period of the day and the same day type as period $T + h$; and λ ($0 \leq \lambda \leq 1$) is a decay parameter. The decay is imposed in steps of size 336, which is the number of half-hours in a week. This ensures that observations from the same week are given equal weighting. For each day in our post-sample period, we implemented the KDE using the previous 3 months of data.

For each series, we selected b and λ by minimizing the continuous ranked probability score (CRPS) (see, for example, Gneiting et al. 2007) for a cross-validation period consisting of the one month immediately prior to our post-sample period. In using cross-validation, we are adopting a

data-driven approach to KDE parameter optimization (see, for example, Hall et al. 2004), rather than a rule-based approach. Since we used a Gaussian kernel function K , we computed the CRPS using the closed-form expression for a mixture of Gaussians (see Grimit et al. 2006). We are not aware of the previous use of this expression for KDE. The selected values of b and λ tended to be quite small, indicating little kernel smoothing and fast decay.

5.2 Forecasting aggregated series

The autocorrelation in the time series of the aggregates (see, for example, Figure 2) motivates the use of a time series model, rather than KDE. For the modeling of the total demand on a transmission system, De Livera et al. (2011) generalize the HWT exponential smoothing model of Taylor (2010, Section 3.1), which models the intraday and intraweek cycles in intraday data, and incorporates an autoregressive model for the residuals. We chose to use this model for the aggregates, rather than the models of De Livera et al. (2011), as these require a selection procedure, which is challenging in our context, where the chosen method must be applied in an automated fashion to many series.

Let y_1, \dots, y_T be one of the aggregate series in the hierarchy. The HWT exponential smoothing model is given by the following expressions:

$$y_t = \ell_{t-1} + d_{t-48} + w_{t-336} + r_t, \quad (15)$$

$$\ell_t = \ell_{t-1} + \alpha r_t, \quad (16)$$

$$d_t = d_{t-1} + \delta r_t, \quad (17)$$

$$w_t = w_{t-1} + \omega r_t, \quad (18)$$

$$r_t = \phi r_{t-1} + \varepsilon_t, \quad (19)$$

where ℓ_t is the smoothed level; d_t is the seasonal index for the intraday pattern; w_t is the seasonal index for the intraweek pattern that remains after the intraday pattern has been removed; α , δ and ω are smoothing parameters; r_t is a residual term that is modeled as a first order autoregressive process with parameter ϕ ; and ε_t is a random noise term with mean zero and finite variance.

We estimated the initial smoothed values for the level and seasonal components of each series by averaging the observations from the first three weeks of data. For each series, we optimized

the parameters by minimizing the sum of squared one step-ahead forecast errors for the first 12 months of data. Table 1 presents the optimized parameter values for the four series of aggregates considered in Figures 2 and 3. These values are similar to those found in previous applications of the model to electricity load (see, for example, Taylor & McSharry 2012), with relatively small values of α and relatively high values of ϕ .

An expression for the forecast of the mean is given by Taylor (2010). We constructed density forecasts using bootstrapping based on the in-sample one step-ahead forecast errors $\{\hat{e}_1, \dots, \hat{e}_T\}$. The bootstrapping proceeded by randomly sampling 48 times from this set of forecast errors. We treat these values as one step-ahead forecast errors for each of the next 48 periods. We express the values as $\{\hat{e}_{T+1}^{(b)}, \dots, \hat{e}_{T+48}^{(b)}\}$, and refer to this as the b th bootstrapped sample, with $b = 1, \dots, B$. Using this sample and the estimated parameters $\hat{\alpha}, \hat{\delta}, \hat{\omega}, \hat{\phi}$ in the model of expressions (15)-(19), we compute a sample path $\{y_{T+1}^{(b)}, \dots, y_{T+48}^{(b)}\}$. We repeat this $B=5000$ times. The empirical distribution of $\{y_{T+h}^{(1)}, \dots, y_{T+h}^{(B)}\}$ is then used as the predictive distribution for y_{T+h} for each lead time $h = 1, \dots, 48$.

The first of the two plots in Figure 5 shows forecasts of the mean, and 50% and 95% prediction intervals produced using the exponential smoothing method for the aggregated series at the top of the hierarchy. The forecasts were produced from the end of the estimation sample of 12 months, for lead times from one half-hour up to 24 hours ahead. In Figure 5, the coverage rates of the 50% and 90% intervals are 48% and 94%, respectively. The second of the plots in Figure 5 shows forecasts of the mean and prediction intervals for the KDE approach for one individual smart meter series. In this figure, the coverage rates of the 50% and 90% intervals are 44% and 83%, respectively.

The simplest approach to hierarchical forecasting is to produce forecasts independently for each node of the hierarchy. In Section 3.1, in relation to expression (3), we referred to these as the base forecasts, and we discussed how they are unlikely to satisfy the aggregation constraint. This is illustrated by Figure 6, which shows boxplots of the resulting base forecast coherency errors, defined in expression (4), computed for each period of the day using the 92-day post-sample period. The two panels correspond to two of the aggregate series considered in Figures 2 and 3. As these are aggregate series, we used the exponential smoothing method to produce forecasts. Naturally, we can see that the magnitude of the coherency errors increases with the amount of aggregation. We can also see that the sum of the bottom level forecasts tends to be higher than the base aggregate

Table 1: Parameters of the exponential smoothing method at different levels of aggregation.

	Number of aggregated meters			
	1578	150	30	10
α	0.007	0.019	0.012	0.017
δ	0.209	0.113	0.083	0.060
ω	0.187	0.090	0.081	0.081
ϕ	0.863	0.597	0.554	0.398

forecasts, especially during the second peak of the day around 19:30.

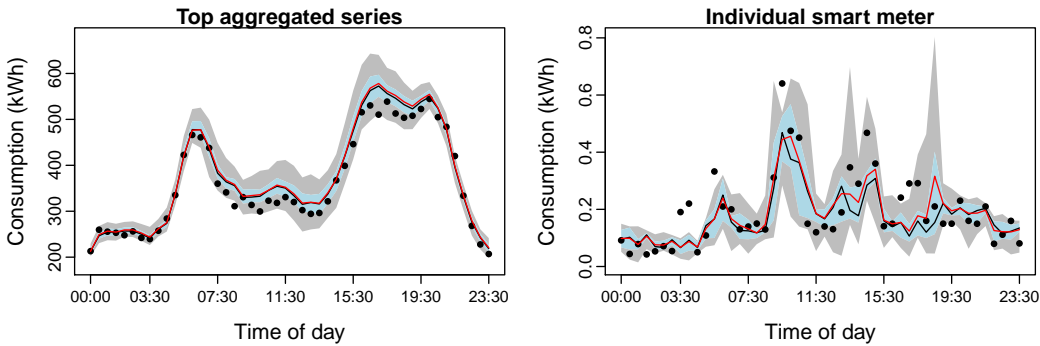


Figure 5: One day ahead probabilistic forecasts for the top aggregated series and one smart meter series, using the exponential smoothing and KDE method, respectively. The central line indicates the forecasts of the mean, and the shaded regions show 50% and 95% prediction intervals.

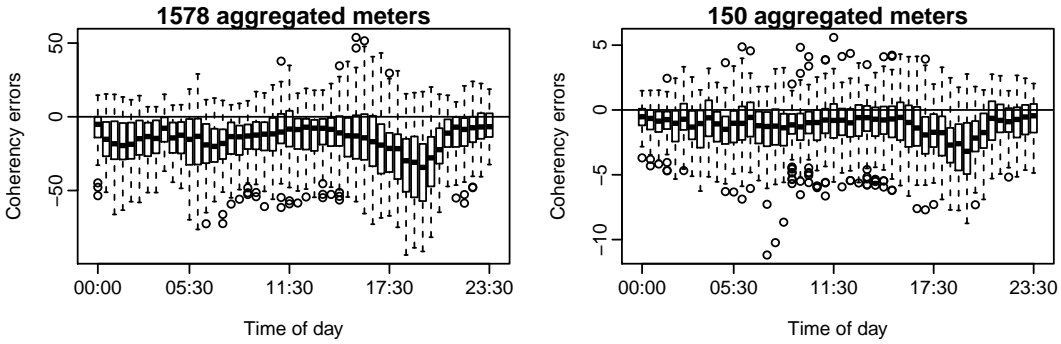


Figure 6: Boxplots of coherency errors for the base forecasts of two aggregated series.

6 Empirical Study of Smart Meter Data

In this section, we empirically evaluate mean and probabilistic hierarchical forecasts. We first describe the evaluation measures that we use, and list the forecasting methods in our study.

6.1 Evaluation measures

To evaluate predictive distributions, we use the CRPS, which is a proper scoring rule, i.e. the score is maximized when the true distribution is reported (Gneiting et al. 2007). The log score is another popular proper score for density forecasts. However, the log score can be difficult to compute, and this was the case in our work, where we generate distributional forecasts for continuous variables from simulated values. As a discrete density is produced, the log score cannot be computed for future outcomes (almost surely). A general concern with the log score is that it takes large values for low-probability events, meaning that it is sensitive to outliers, leading Gneiting et al. (2007) to conclude that the CRPS is an attractive alternative.

We also use the weighted form of the CRPS, which allows more emphasis to be put on probability levels of greater interest (Gneiting & Ranjan 2011). Given an h period-ahead predictive distribution \hat{F}_{t+h} and an observation y_{t+h} , the quantile-weighted version of the CRPS is

$$\text{CRPS}(\hat{F}_{t+h}, y_{t+h}) = \int_0^1 v(\tau) \text{QS}_\tau(\hat{F}_{t+h}^{-1}(\tau), y_{t+h}) d\tau, \quad (20)$$

where $v(\tau)$ is a non-negative weight function on the unit interval, and QS_τ is the quantile score at probability level τ , defined as

$$\text{QS}_\tau(\hat{F}_{t+h}^{-1}(\tau), y_{t+h}) = 2 \left(\mathbb{1}\{y_{t+h} \leq \hat{F}_{t+h}^{-1}(\tau)\} - \tau \right) (\hat{F}_{t+h}^{-1}(\tau) - y_{t+h}).$$

When closed-form expressions for the evaluation of expression (20) are not available, a discretized approximate version can be computed to any degree of accuracy. In our use of the weighted CRPS, we set $v(\tau) = (2\tau - 1)^2$, which gives more weight to the tails of the distribution.

We averaged the CRPS across the 92 days in our post-sample period. Although our main focus is probabilistic forecasting, we also evaluate forecasts of the mean. For this, we use the root mean squared error (RMSE), as this is a proper scoring rule for the mean (Gneiting 2011).

For conciseness, when presenting the results, we report the average of the scores for the periods of the day split into three eight-hour intervals. For ease of comparison, we present skill scores. These measure the performance relative to a reference method. In our application, a natural reference is the base forecasts, which are produced independently for each series in the hierarchy. For each method, to calculate the skill score, we compute the ratio of the score to that of the base forecasts, then subtract this ratio from one, and multiply the result by 100. The skill score, therefore, conveys the percentage by which a method's score is superior to the score of the reference method.

6.2 Forecasting methods

For each half-hour of each of the 92 days in our post-sample period, we made predictions from 23:30 of the previous day. This implies 48 different lead times. We computed predictive distributions using the following seven methods:

1. BASE - We independently produce predictive distributions for each node in the hierarchy. For each bottom level series, we use the KDE method described in Section 5.1, and for each aggregate series, we use the exponential smoothing model of Section 5.2. This BASE method is used as the reference in the calculation of the skill scores.
2. LogN-MinTDiag - Forecasts of the means and variances for each node are computed using the MinT expressions (8) and (6), respectively. A diagonal covariance matrix \mathbf{W}_h is used within the method, which led us to label this method MinTDiag in Section 3.2. Forecasts of the probability distributions are produced by assuming log-normality.
3. LogN-MinTShrink - This is identical to LogN-MinTDiag, except that a shrunken covariance matrix \mathbf{W}_h is used within the MinT method. We referred to this version of the MinT method as MinTShrink in Section 3.2.
4. IndepBU-NoMinT - In this bottom-up approach, we compute the aggregate forecasts by Monte Carlo simulation. Predictive distributions for the aggregates are generated from the sum of independently sampled values of the predictive distributions, produced by the BASE method, for the bottom level nodes.

5. IndepBU-MinTShrink - This is identical to IndepBU-NoMinT, except that, prior to the Monte Carlo simulation, the MinTShrink method is used to revise the predictive distributions produced by the BASE method for the nodes in the bottom level.
6. DepBU-NoMinT - In this bottom-up approach, we impose dependency on the IndepBU-NoMinT method. Simulation is again used. We compute the aggregate forecasts by summing permuted independently sampled values from the predictive distributions, produced by the BASE method, for the bottom level nodes. In other words, we use our algorithm of Section 4.5 with $\tilde{F}_{i,T+h} = \hat{F}_{i,T+h}$ in expression (13). Note that the predictive means are equal for IndepBU-NoMinT and DepBU-NoMinT. This is because they reduce to simple bottom-up mean forecasts, given by expression (2).
7. DepBU-MinTShrink - This is identical to DepBU-NoMinT, except that, in an initial step, the MinTShrink method is used to revise the predictive distributions produced by the BASE method for the nodes in the bottom level.

Although previous literature has not considered any of these seven methods for probabilistic hierarchical forecasting, we should acknowledge that the BASE method is a simple benchmark, and that the methods involving MinTDiag and MinTShrink are founded on the work of Wickramasuriya et al. (2018), who consider hierarchical forecasting for the mean. The BASE method is typically neither mean or probabilistically coherent, and the MinT approaches require a distributional assumption. These issues motivate our use of a bottom-up approach based on Monte Carlo simulation, and we include four of these in our empirical study. While the IndepBU-NoMinT method can also be considered as a relatively simple benchmark, the IndepBU-MinTShrink method is more novel and sophisticated, with our aim being to incorporate, within a simple bottom-up approach, the MinT approach to hierarchical forecasting of the mean. However, it is important to note that our main methodological contribution is the DepBU-MinTShrink method, which is the algorithm described in Section 4.5. A simplified version of this is DepBU-NoMinT, which is also new.

6.3 Hierarchical mean forecasting

For different times of the day, Figure 7 presents the RMSE values and Figure 8 shows RMSE skill scores of different methods for aggregates constructed from different numbers of meters. As

we mentioned in the previous section, mean forecasts are the same from IndepBU-NoMinT and DepBU-NoMinT, and so we use the simple label NoMinT for the results of these methods in Figures 7 and 8. Similarly, the mean forecasts from LogN-MinTShrink, IndepBU-MinTShrink and DepBU-MinTShrink are the same, and so we use the label MinTShrink for these methods. The label MinTDiag refers to the mean forecasts from LogN-MinTDiag.

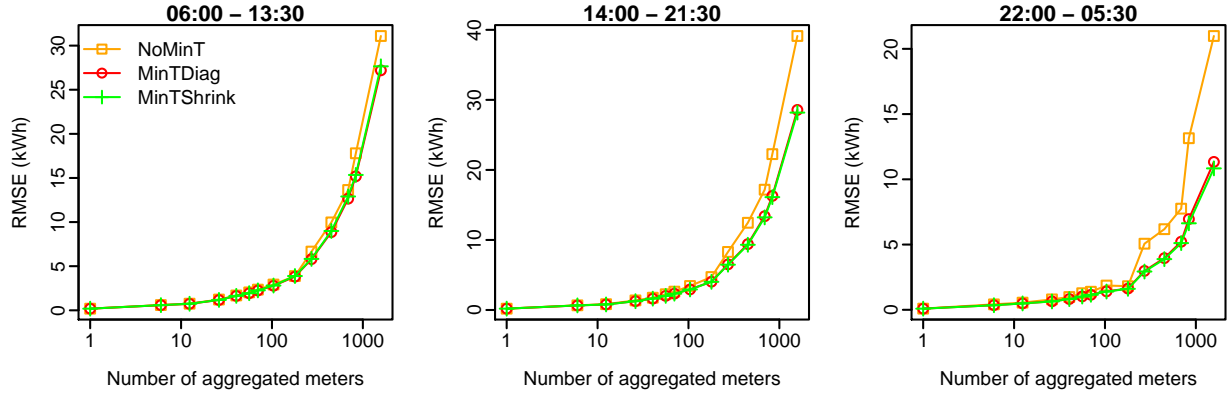


Figure 7: RMSE at different periods of the day for aggregates of different numbers of meters.

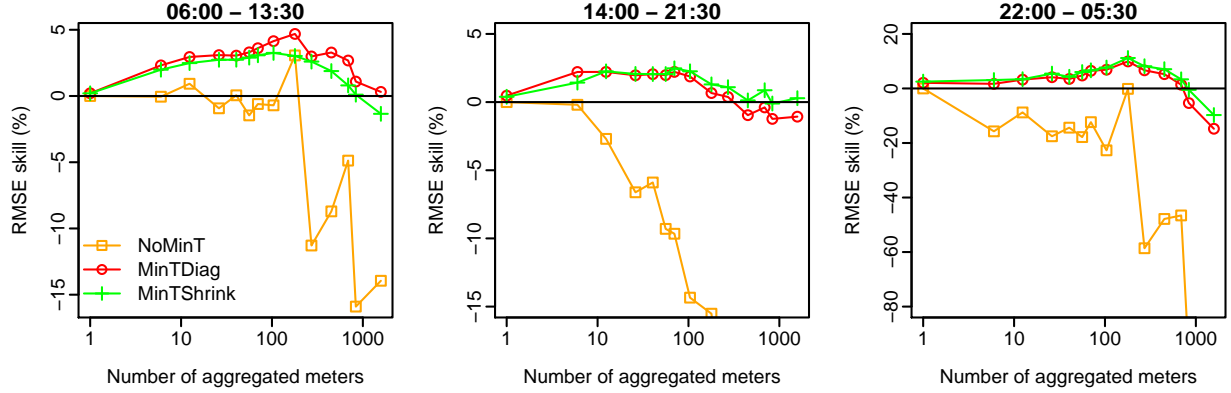


Figure 8: RMSE skill scores at different periods of the day for aggregates of different numbers of meters.

For NoMinT, Figure 8 shows negative skill scores at both intermediate and large aggregations, and this is consistent across different time periods. In other words, aggregate forecasts obtained by simply summing the smart meter (bottom level) forecasts are poor compared to the base forecasts. This can be explained by the low signal-to-noise ratio at the smart meter level. By contrast, for the aggregate series, the BASE method has the advantage of using the observations for the aggregates, which are smoother. The lack of forecast accuracy for a bottom-up approach has also

been observed in many other applications (Hyndman et al. 2011). Although BASE dominates the NoMinT methods, i.e. IndepBU-NoMinT and DepBU-NoMinT, BASE has the disadvantage of not producing coherent forecasts, while the bottom-up forecasts are coherent by construction.

In Figure 8, the methods involving MinT perform well. The positive skill scores for these methods shows that they provide better forecasts than BASE at intermediate aggregations. Recall that all MinT methods are bottom-up procedures, but with an additional forecast combination step. The improvement in forecast accuracy, in comparison with the NoMinT methods, shows the effectiveness of including forecast combination in a bottom-up procedure. The relative performance of MinTDiag and MinTShrink in Figure 8 depends on the time of day, and the level of aggregation. Recall that, in contrast to MinTShrink, MinTDiag ignores the correlation between the forecast errors at different nodes in the hierarchy. The relative performance of these two methods will depend on the correlation structure of the base forecast errors, and this will vary across the times of the day and levels of aggregation. To summarize this section with regard to our proposed method, DepBU-MinTShrink, the results are encouraging, as it is one of the MinTShrink methods.

6.4 Hierarchical probabilistic forecasting

Figures 7 and 8 showed that IndepBU-NoMinT and DepBU-NoMinT produced poor forecasts of the mean for the aggregates. This was also the case with the density forecasts from these methods, which is not surprising, as the accuracy of any density forecast is typically heavily dependent on the accuracy of the forecast of the location of the density. In view of this, for brevity, in this section, we focus on the other methods in our discussion of the probabilistic forecasting results.

Figures 9 and 10 report the CRPS and weighted CRPS skill scores for DepBU-MinTShrink, IndepBU-MinTShrink, LogN-MinTDiag and LogN-MinTShrink. In Figure 9, LogN-MinTDiag is noticeably poorer than LogN-MinTShrink, especially for large aggregations. This contrasts with the results in Figures 7 and 8 for forecasts of the mean. This is not surprising, as the error correlations directly affect the variance, and hence the predictive distributions, but have only a second-order effect on the mean. The weighted CRPS results of Figure 10 show an even larger difference between LogN-MinTDiag and LogN-MinTShrink, indicating that capturing the correlation has a particularly strong impact on distributional tail accuracy.

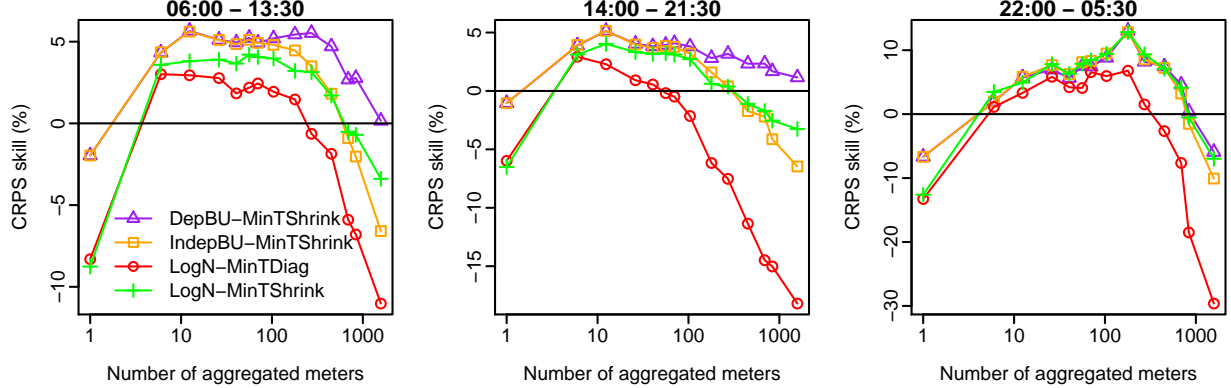


Figure 9: CRPS skill scores at different periods of the day for aggregates of different numbers of meters.

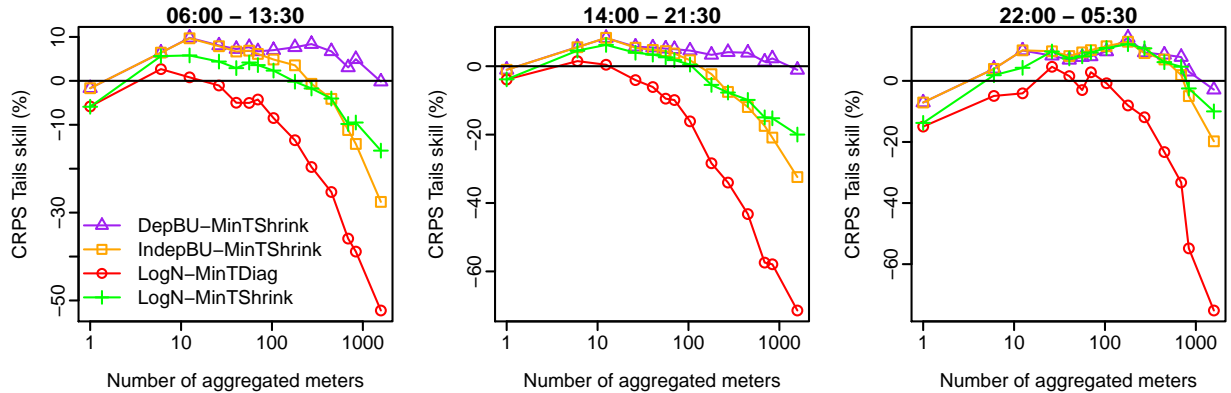


Figure 10: Weighted CRPS skill scores at different periods of the day for aggregates of different numbers of meters.

It is interesting to see that IndepBU-MinTShrink, which involves an independence assumption, sometimes has better skill scores than LogN-MinTShrink which models the full covariance matrix. While LogN-MinTShrink uses a log-normality assumption for the bottom level nodes, IndepBU-MinTShrink seemingly has the advantage of using a nonparametric approach for these nodes.

Our proposed method, DepBU-MinTShrink, has better skill scores than IndepBU-MinTShrink and LogN-MinTShrink during day hours, and similar or slightly better skill scores during night hours. The negative skill scores for all methods at the bottom level suggests that the mean forecast combination does not improve the CRPS with respect to the base forecasts at that level.

The positive skill scores for DepBU-MinTShrink indicate that it provides better forecasts than BASE at almost all aggregations and times of the day. The fact that this is achieved, while the method is a bottom-up procedure, suggests that our algorithm is effective in providing both coher-

ent and accurate probabilistic forecasts. We acknowledge that the DepBU-MinTShrink skill scores are negative for the bottom-level series. However, these negative values are quite small, and reflect the difficulty in computing the MinT combination weights for the bottom-level series.

We also evaluated the coverage of 50% and 90% prediction intervals produced by each method for the series at each node in the hierarchy. For each of the seven methods considered in our study, each boxplot in the left panel in Figure 11 summarizes the different coverage rates that we obtained for the series at all levels of the hierarchy, except the bottom level. This figure shows a variety of performances among the methods, with our proposed method DepBU-MinTShrink performing particularly well for the 90% intervals. Each boxplot in the right panel of Figure 11 summarizes the different coverage rates that we obtained for the bottom level series. For the 90% intervals, the figure shows reasonable performance for all seven methods. For the 50% intervals, the results are poor for only the two methods based on the log normal distribution, which confirms that this parametric assumption is inadvisable.

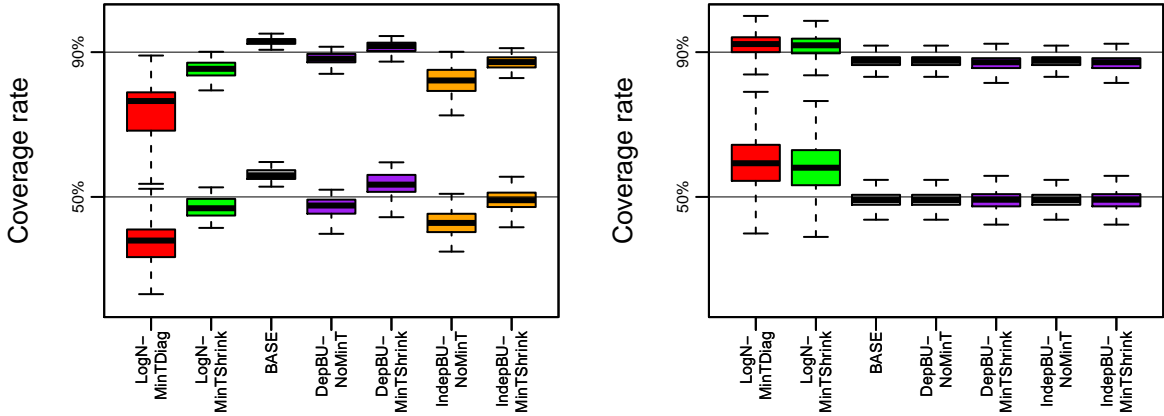


Figure 11: Boxplots summarizing coverage rates for 50% and 90% prediction intervals produced by each method for each node in the aggregated levels (left panel) and bottom level (right panel).

6.5 Discussion

In the context of managing electricity supply, decisions must be made regarding the quantity of generation and its distribution across the power grid. Supply must be sufficient to meet anticipated demand, as inadequate or unreliable supply can be costly for individuals and organisations, as well as inconvenient and sometimes dangerous. Of course, overprovision of electricity also has cost

implications, as electricity cannot easily be stored on a large scale, and there are important environmental concerns when generation is sourced from fossil fuels. Electricity demand is inherently uncertain, and particularly so at less aggregated demand points, such as the consumption recorded by residential smart meters, as shown in Figure 2. This uncertainty must be taken into consideration when making supply decisions. In other words, probabilistic forecasts for demand at different points in the power grid are required since they are essential for optimal decision making (Gneiting & Katzfuss 2014).

As we discussed with respect to Figure 1, it is natural to view the forecasting of electricity consumption as a hierarchical forecasting problem. The literature in this area has emphasised the need for forecast coherency. For our application, this is important from a practical perspective, because decisions regarding the allocation of electricity at one level of the hierarchy rely on sufficient electricity being provided from the previous level, and this is unlikely if forecasts at the different levels are not coherent in a statistical sense. An important feature of our method is that it delivers a hierarchy of probabilistic forecasts that are coherent. By contrast, Figure 6 shows that this is not a feature of the base forecasting method.

Coherency can be ensured by using a simple bottom-up forecasting method. However, as our results in Figure 8 show, this approach provides poor forecast accuracy. Base forecasting is far more accurate, but it is a practical concern that it does not deliver a set of coherent forecasts for the hierarchy. Our results in Figures 8 and 10 show that our method successfully builds on the base forecasts by, in a sense, drawing on the ‘wisdom of the crowd’ of forecasts in the hierarchy, to deliver improvements in accuracy, while ensuring coherency. Our results also confirm the importance of avoiding distributional assumptions, which is important for an electricity demand hierarchy, where highly disaggregated data is typically more positively skewed than aggregated data. In terms of computational feasibility, any forecasting approach for this application only has practical relevance if it is scalable, and this was an important feature in the design of our method.

7 Empirical Study of Simulated Data

In this section, we describe a simulation study that we used to analyze how well each hierarchical forecasting method captures the true distribution under different data conditions. Our simulation

design was based on the study in Section 3.2 of Wickramasuriya et al. (2018), who focused on point forecasting. We adjusted and extended that study to probabilistic forecasting.

Our hierarchy consisted of three levels with 126 series in total. More specifically, 100 series at the bottom level were aggregated in groups of four for the next level, resulting in 25 series. These 25 series were then aggregated to obtain the top level series.

Each series in each group of four was generated from an ARMA(p, q) process with p and q set equal to 0, 1 and 2, with equal probability. The parameters were chosen randomly from a uniform distribution over a space well within the stationary and invertible parameter space (see Table 1 in Wickramasuriya et al. 2018). For the random error terms, we used a Gaussian distribution¹. To induce dependences between the series, we used a four-dimensional Gaussian copula with a covariance matrix that allowed a strongly positive error dependency among the series within each group of four bottom level series, but only moderately positive dependency between bottom level series from different groups.

The bottom level series were first generated, and then summed to obtain the series for the levels above. We considered both a short and long time series, namely $T = 500$ and $T = 10,000$. We focused on one-step-ahead prediction for period $T+1$. For the purpose of evaluating distributional forecasts, we obtained a sample of 1000 simulated values from the true distribution, for period $T+1$, at each node of the hierarchy. To achieve this, we proceeded by simulating a value from each bottom level series for period $T+1$, and then summing appropriately to obtain the value for each series in the levels above. Doing this 1000 times delivered the sample of simulated values from the true distribution in period $T+1$ at each node.

For each series in the hierarchy, the base forecasts were generated using an ARMA model fitted using the automated algorithm of Hyndman & Khandakar (2008), which is implemented in the *forecast* package for R (Hyndman 2017). The one-step ahead predictive distributions were generated by bootstrapping the residuals. We felt that inaccuracy in the base forecasts at the bottom level might limit insight regarding the hierarchical probabilistic forecasting methods. In view of this, we ran our simulation experiments in two different ways. First, for the base forecasts at the bottom level, we used the true lag order and parameters from the ARMA data generating processes.

¹We also considered a Student's t distribution with six degrees of freedom, but this did not lead to notably more insight. The details are given in Appendix A in the supplementary materials.

We could not repeat this for the series in the higher levels, as the parameters of the true data generating processes for these levels is unknown. Our second run of the simulation experiments used estimated ARMA parameters to produce forecasts for each series in the hierarchy.

To produce probabilistic forecasts for the full hierarchy, we implemented the seven methods listed in Section 6.2. For the two methods that included a log normal distribution in Section 6.2, we instead used a Gaussian distribution in our simulation study. We refer to these two methods as Norm-MinTDiag and Norm-MinTShrink.

For each series, given a sample from the predictive distribution and a sample from the true distribution, we performed a two-sample Kolmogorov–Smirnov (KS) test, for which the null hypothesis is that the two samples are drawn from the same distribution. We repeated this for each of 1000 simulated hierarchies. Each panel in Figures 12a and 12b gives boxplots of the resulting p-values for the case where we used true ARMA parameters to produce the bottom level forecasts. Under the null hypothesis, the p-values are uniformly distributed. Uniformity is, therefore, the ideal result. In each figure, the first of the four panels is for the top-level series, the second panel is for one series in the second level, and the third panel is for one series in the bottom level.

By comparing the third panels of Figures 12a and 12b, i.e. the bottom level of the hierarchy, we can see that all methods capture the true distribution better when the time series length is increased from $T = 500$ to $T = 10,000$. Note that the bottom level forecasts from IndepBU-NoMinT and DepBU-NoMinT are equal to the base forecasts. The first and second panels show that for the upper levels of the hierarchy, regardless of the time series length, performance was poor for the three methods that do not model the dependences between the series in the bottom level, i.e. Norm-MinTDiag, IndepBU-NoMinT and IndepBU-MinTShrink. In Figure 12b, the impressive performance of Norm-MinTShrink can be explained by the method’s distributional assumption being the same as the error of the data generating process. The DepBU-NoMinT method and our proposed DepBU-MinTShrink method involve no distributional assumption, as they are nonparametric, and so it is encouraging that they also performed well.

As we indicated previously, the results of Figures 12a and 12b correspond to the case where we used true ARMA parameters to produce the bottom level forecasts. Figures 13a and 13b are the analogous results for the case where we used estimated ARMA parameters to produce forecasts for each series in the hierarchy. These results are similar to those in Figures 12a and 12b, with the

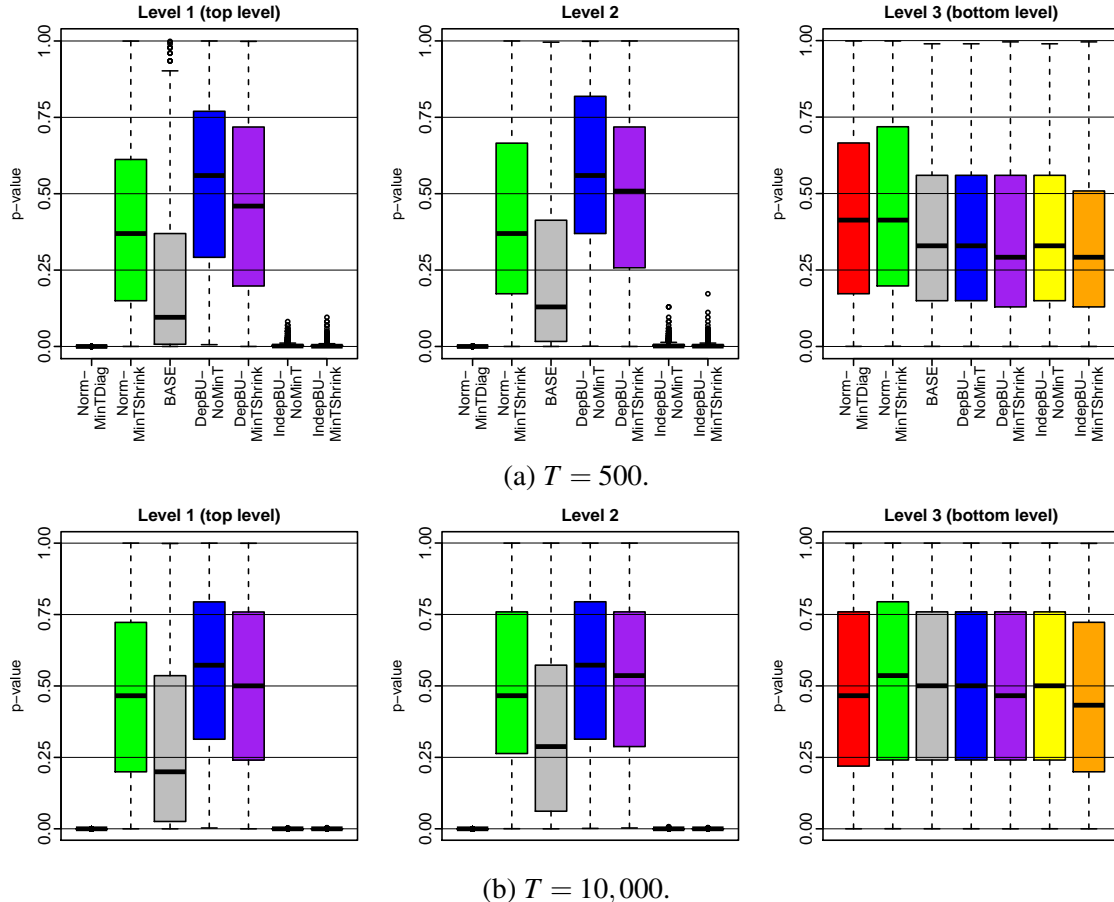


Figure 12: Data simulated using normally distributed errors. Boxplot of p-values associated with a K-S test for different hierarchical forecasting methods. *True* ARMA parameters are used to forecast series in the bottom level.

only notable difference being the poorer results for the bottom level series. It was to be expected that the bottom level series would be better modeled using the true ARMA parameters, but it is interesting to see how little effect parameter estimation error had on prediction in the upper levels.

We also evaluated the seven hierarchical methods in terms of the closeness of each predictive distribution to the simulated distribution, constructed at each node by the 1000 simulated values for period $T+1$. We measured this using the L_2 -Wasserstein distance (Ramdas et al. 2017) for each of the 1000 simulated hierarchies. Lower values of this distance measure are preferable. Figure 14 summarizes the resulting values using boxplots for the case of estimated ARMA parameters. The rankings of methods in this figure is similar to the rankings in Figures 13a and 13b for the KS test results.

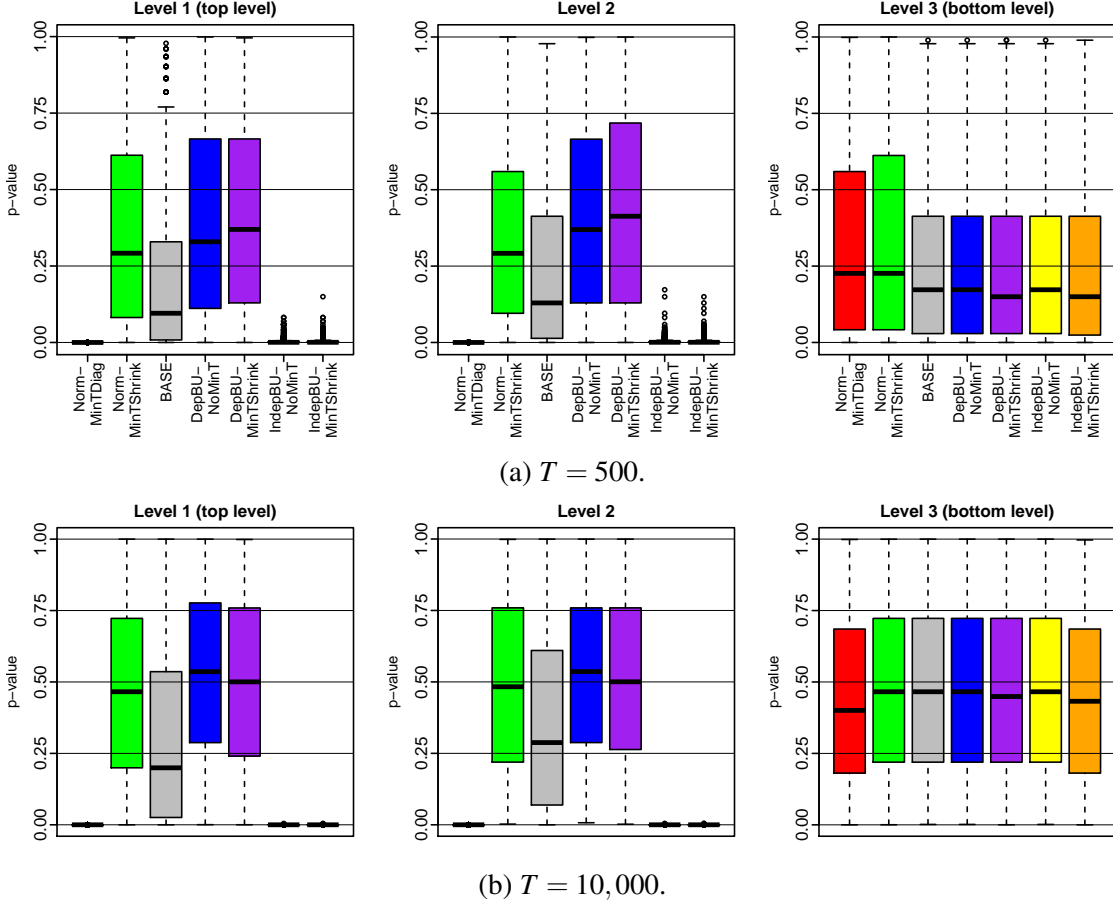


Figure 13: Data simulated using normally distributed errors. Boxplot of p-values associated with a K-S test for different hierarchical forecasting methods. The ARMA parameters are estimated from data.

8 Conclusion

Modern electricity networks provide remarkably rich sources of data at a highly disaggregated level. As with many “big data” problems, the richness of the data set presents some new and interesting statistical challenges. We have focused on one such challenge, namely the problem of computing coherent probabilistic forecasts for a hierarchy of electricity consumption time series.

While previous considerations of hierarchical forecasting have focused on ensuring that the mean forecasts are coherent, we have tackled the more challenging problem of obtaining probabilistically coherent forecast distributions. In fact, we have exploited recent results to ensure the means of our probability distributions are not only coherent but efficiently use all available information. In principle, coherent forecast distributions require the estimation of the entire joint

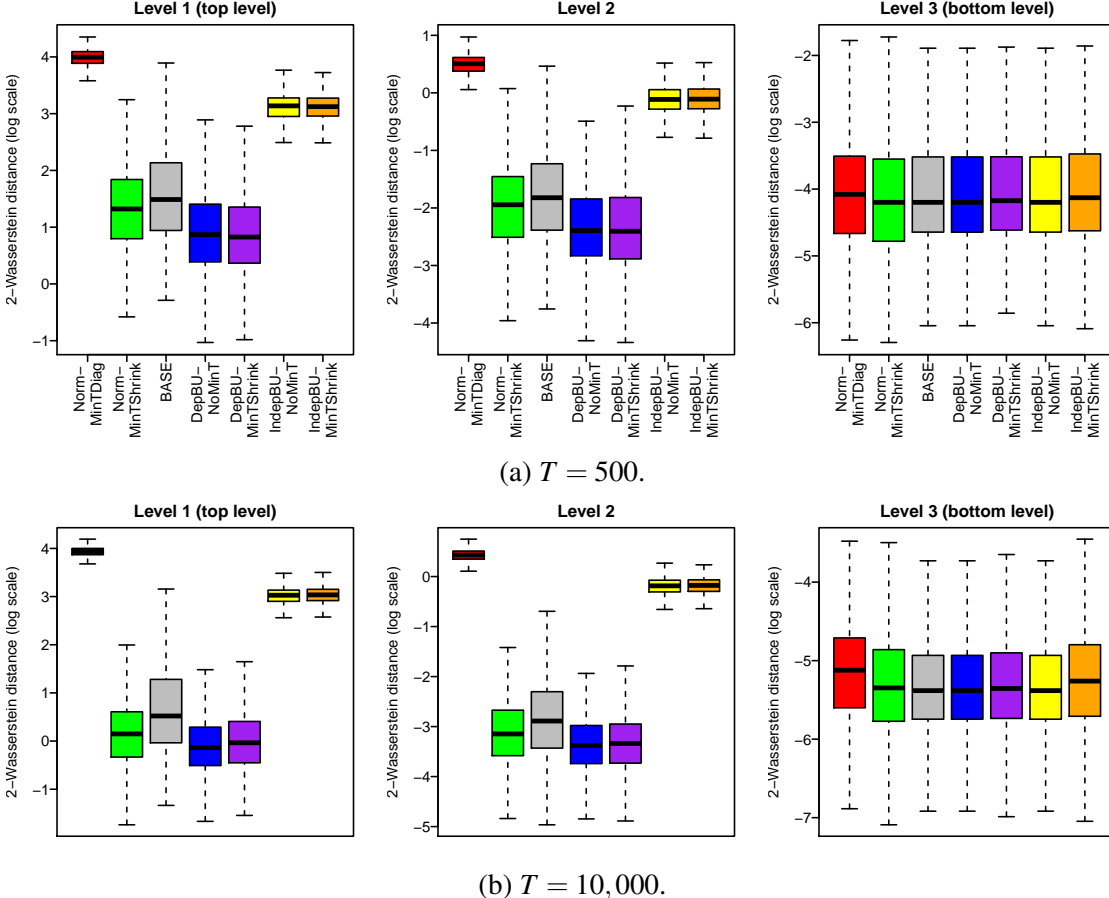


Figure 14: Data simulated using normally distributed errors. Boxplot of L_2 -Wasserstein distances computed between a sample from the true data generating process and a sample from the predictive distribution for 1000 simulations. The ARMA parameters are estimated from data.

distribution of all the bottom-level time series. To circumvent this problem, we exploit the hierarchical structure of the data, allowing us to reduce the problem to smaller sub-problems, each of which is computationally tractable. Another feature of our approach is that we make no assumptions about the underlying distributions, using conditional KDE for the smart meter time series, and using fast time series models that handle the multiple seasonal patterns observed in the aggregated data. For our smart meter data, overall, the best performing method involves mean forecast combination using a shrinkage estimator for the covariance matrix of the one-step forecast errors, and our copula-based approach for computing the predictive distributions of all nodes in the hierarchy.

Although we have focused on electricity demand, our work is applicable to other contexts, such as sales product hierarchies, or tourist numbers in geographical hierarchies. In addition to considering such applications, we are interested in adapting our approach for count data, and de-

veloping an approach based on Bayesian hierarchical modeling, which would have the appeal of the Bayesian framework, although the need for parametric assumptions is likely. In this paper, non-parametric approaches have featured heavily with KDE for the base forecasting of the bottom level series, an empirical distribution used with the exponential smoothing forecasts, and an empirical copula employed within our algorithm. These methods are reasonable for situations, such as ours, where quite long time series are available. However, for short series, these approaches are likely to be improved with the use of parametric methods, and this would be an interesting area of future research. In terms of a parametric method for base forecasting, it would be interesting to consider dynamic factor models or sparse vector autoregressive models (see Bessa et al. (2015); Dowell & Pinson (2016)), although dimensionality is likely to be a challenge. It would also be interesting to consider applications with significant missing observations. Missing observations can be particularly challenging for hierarchical forecasting when the series have missing values in different periods, leading to an accumulation of missing values in the aggregate series. A further area of interest is the use of our approach within a procedure for optimizing the hierarchy architecture (see Misiti et al. (2010)).

Acknowledgments

We are very grateful to the Editor, an associate editor and three referees for providing very useful comments on the paper.

References

- AECOM (2011), Energy demand research project: Final analysis, Technical report, AECOM House, Hertfordshire, UK.
- AECOM Building Engineering (2014), ‘Energy demand research project: Early smart meter trials, 2007–2010’, <http://doi.org/10.5255/UKDA-SN-7591-1>.
- Arbenz, P., Hummel, C. & Mainik, G. (2012), ‘Copula based hierarchical risk aggregation through sample reordering’, *Insurance, Mathematics & Economics* **51**(1), 122–133.
- Arora, S. & Taylor, J. W. (2016), ‘Forecasting electricity smart meter data using conditional kernel density estimation’, *Omega* **59, Part A**, 47–59.
- Ben Taieb, Huser, R., Hyndman, R. J. & Genton, M. G. (2016), ‘Forecasting uncertainty in electricity smart meter data by boosting additive quantile regression’, *IEEE Transactions on Smart Grid* **7**(5), 2448–2455.

- Berrocal, V. J., Raftery, A. E., Gneiting, T. & Steed, R. C. (2010), ‘Probabilistic weather forecasting for winter road maintenance’, *Journal of the American Statistical Association* **105**(490), 522–537.
- Bessa, R. J., Trindade, A. & Miranda, V. (2015), ‘Spatial-Temporal solar power forecasting for smart grids’, *IEEE Transactions on Industrial Informatics* **11**(1), 232–241.
- Borenstein, S. & Bushnell, J. (2015), ‘The US electricity industry after 20 years of restructuring’, *Annual Review of Economics* **7**(1), 437–463.
- Borges, C. E., Penya, Y. K. & Fernandez, I. (2013), ‘Evaluating combined load forecasting in large power systems and smart grids’, *IEEE Transactions on Industrial Informatics* **9**(3), 1570–1577.
- Cabrera, B. L. & Schulz, F. (2017), ‘Forecasting generalized quantiles of electricity demand: A functional data approach’, *Journal of the American Statistical Association* **112**(517), 127–136.
- Cho, H., Goude, Y., Brossat, X. & Yao, Q. (2013), ‘Modeling and forecasting daily electricity load curves: A hybrid approach’, *Journal of the American Statistical Association* **108**(501), 7–21.
- Cottet, R. & Smith, M. (2003), ‘Bayesian modeling and forecasting of intraday electricity load’, *Journal of the American Statistical Association* **98**(464), 839–849.
- De Livera, A. M., Hyndman, R. J. & Snyder, R. (2011), ‘Forecasting time series with complex seasonal patterns using exponential smoothing’, *Journal of the American Statistical Association* **106**(496), 1513–1527.
- Dowell, J. & Pinson, P. (2016), ‘Very-Short-Term probabilistic wind power forecasts by sparse vector autoregression’, *IEEE Transactions on Smart Grid* **7**(2), 763–770.
- Gijbels, I. & Herrmann, K. (2014), ‘On the distribution of sums of random variables with copula-induced dependence’, *Insurance, Mathematics & Economics* **59**, 27–44.
- Gneiting, T. (2011), ‘Making and evaluating point forecasts’, *Journal of the American Statistical Association* **106**(494), 746–762.
- Gneiting, T., Balabdaoui, F. & Raftery, A. E. (2007), ‘Probabilistic forecasts, calibration and sharpness’, *Journal of the Royal Statistical Society. Series B, Statistical methodology* **69**(2), 243–268.
- Gneiting, T. & Katzfuss, M. (2014), ‘Probabilistic forecasting’, *Annual Review of Statistics and Its Application* **1**(1), 125–151.
- Gneiting, T. & Ranjan, R. (2011), ‘Comparing density forecasts using threshold- and Quantile-Weighted scoring rules’, *Journal of Business & Economic Statistics* **29**(3), 411–422.
- Grimit, E. P., Gneiting, T., Berrocal, V. J. & Johnson, N. A. (2006), ‘The continuous ranked probability score for circular variables and its application to mesoscale forecast ensemble verification’, *Quarterly Journal of the Royal Meteorological Society* **132**(621C), 2925–2942.
- Haben, S., Ward, J., Vukadinovic Greetham, D., Singleton, C. & Grindrod, P. (2014), ‘A new error measure for forecasts of household-level, high resolution electrical energy consumption’, *International Journal of Forecasting* **30**(2), 246–256.
- Hall, P., Racine, J. & Li, Q. (2004), ‘Cross-Validation and the estimation of conditional probability densities’, *Journal of the American Statistical Association* **99**(468), 1015–1026.
- Hong, T., Pinson, P., Fan, S., Zareipour, H., Troccoli, A. & Hyndman, R. J. (2016), ‘Probabilistic energy forecasting: Global energy forecasting competition 2014 and beyond’, *International Journal of Forecasting*

- ing **32**(3), 896–913.
- Hyndman, R. J. (2017), ‘forecast: Forecasting functions for time series and linear models’.
- Hyndman, R. J., Ahmed, R. A., Athanasopoulos, G. & Shang, H. L. (2011), ‘Optimal combination forecasts for hierarchical time series’, *Computational statistics & data analysis* **55**(9), 2579–2589.
- Hyndman, R. J. & Khandakar, Y. (2008), ‘Automatic time series for forecasting: the forecast package for R’, *Journal of Statistical Software* **27**(3), 1–22.
- Hyndman, R. J., Lee, A. J. & Wang, E. (2016), ‘Fast computation of reconciled forecasts for hierarchical and grouped time series’, *Computational Statistics & Data Analysis* **97**, 16–32.
- Iman, R. L. & Conover, W. J. (1982), ‘A distribution-free approach to inducing rank correlation among input variables’, *Communications in Statistics - Simulation and Computation* **11**(3), 311–334.
- Jeon, J. & Taylor, J. W. (2012), ‘Using conditional kernel density estimation for wind power density forecasting’, *Journal of the American Statistical Association* **107**(497), 66–79.
- Kremer, M., Siemsen, E. & Thomas, D. J. (2016), ‘The sum and its parts: Judgmental hierarchical forecasting’, *Management Science* **62**(9), 2745–2764.
- Mainik, G. (2015), ‘Risk aggregation with empirical margins: Latin hypercubes, empirical copulas, and convergence of sum distributions’, *Journal of Multivariate Analysis* **141**, 197–216.
- Mirowski, P., Chen, S., Ho, T. K. & Yu, C.-N. (2014), ‘Demand forecasting in smart grids’, *Bell Labs Technical Journal* **18**(4), 135–158.
- Misiti, M., Misiti, Y., Oppenheim, G. & Poggi, J.-M. (2010), ‘Optimized clusters for disaggregated electricity load forecasting’, *REVSTAT–Statistical Journal* **8**(2), 105–124.
- Nelsen, R. B. (2007), *An introduction to copulas*, Springer Science & Business Media.
- Patton, A. J. (2006), ‘Modelling asymmetric exchange rate dependence’, *International Economic Review* **47**(2), 527–556.
- Ramchurn, S. D., Vytelingum, P., Rogers, A. & Jennings, N. R. (2012), ‘Putting the ’smarts’ into the smart grid: a grand challenge for artificial intelligence’, *Communications of the ACM* **55**(4), 86–97.
- Ramdas, A., Trillos, N. G. & Cuturi, M. (2017), ‘On wasserstein Two-Sample testing and related families of nonparametric tests’, *Entropy* **19**(2), 47.
- Rüschedorf, L. (2009), ‘On the distributional transform, sklar’s theorem, and the empirical copula process’, *Journal of Statistical Planning and Inference* **139**(11), 3921–3927.
- Schäfer, J. & Strimmer, K. (2005), ‘A shrinkage approach to large-scale covariance matrix estimation and implications for functional genomics’, *Statistical Applications in Genetics and Molecular Biology* **4**, 32.
- Scheuflik, R., Thorarinsdottir, T. L. & Gneiting, T. (2013), ‘Uncertainty quantification in complex simulation models using ensemble copula coupling’, *Statistical science: a review journal of the Institute of Mathematical Statistics* **28**(4), 616–640.
- Sklar, M. (1959), *Fonctions de répartition à n dimensions et leurs marges*, Université Paris 8.
- Smith, M., Min, A., Almeida, C. & Czado, C. (2010), ‘Modeling longitudinal data using a Pair-Copula decomposition of serial dependence’, *Journal of the American Statistical Association* **105**(492), 1467–1479.
- Sun, X., Luh, P. B., Cheung, K. W., Guan, W., Michel, L. D., Venkata, S. S. & Miller, M. T. (2016), ‘An

- efficient approach to Short-Term load forecasting at the distribution level', *IEEE Transactions on Power Systems* **31**(4), 2526–2537.
- Taylor, J. W. (2010), 'Exponentially weighted methods for forecasting intraday time series with multiple seasonal cycles', *International Journal of Forecasting* **26**(4), 627–646.
- Taylor, J. W. & Buizza, R. (2002), 'Neural network load forecasting with weather ensemble predictions', *IEEE Transactions on Power Systems* **17**(3), 626–632.
- Taylor, J. W. & McSharry, P. (2012), Univariate methods for Short-Term load forecasting, in M. El-Hawary, ed., 'Advances in Electric Power and Energy; Power Systems Engineering, Power Engineering Series of IEEE Press', Wiley.
- van Erven, T. & Cugliari, J. (2015), Game-Theoretically optimal reconciliation of contemporaneous hierarchical time series forecasts, in 'Modeling and Stochastic Learning for Forecasting in High Dimensions', Lecture Notes in Statistics, Springer International Publishing, pp. 297–317.
- Wickramasuriya, S. L., Athanasopoulos, G. & Hyndman, R. J. (2018), 'Optimal forecast reconciliation for hierarchical and grouped time series through trace minimization', *Journal of the American Statistical Association* pp. 1–45.